*Author Version of : Marine Pollution Bulletin, vol.172; 2021; Article no: 112892*

# Fate of MV Wakashio oil spill off Mauritius coast through modelling and remote sensing observations

**K. Gurumoorthi, V. Suneel[*], V. Trinadha Rao, Antony P. Thomas, and M. J. Alex**
CSIR-National Institute of Oceanography, Dona Paula -403 004, Goa, India.
[*]Corresponding author: V. Suneel, CSIR-National Institute of Oceanography,
Dona Paula, Goa 403004, India.
Email: suneel@nio.org, Tel +91 832 2450748; Fax No. +91 832 2450608

## Abstract

This study aims at assessing the fate of *MV Wakashio* oil spill, and the driving forces responsible for possible environmental consequences of polluted coastal region. GNOME simulations were performed, considering various meteo-oceanographic forcings such as (i) winds and currents, (ii) only winds, and (iii) only winds with different diffusion coefficients, and validated with the satellite images. The results revealed that the simulations performed with 'only winds' reasonably match with the satellite observations, indicating that winds are the primary driving forces. The conducive stokes drift is an added contribution to the predominant northwestward drift of the spill**.** The oil budget analysis suggests that beaching and evaporation together accounted for a significant portion of the spilled oil (1000 tons), in which ~60% of the oil was accounted only for beaching. Our results depict that the diffusion coefficient of 100,000cm$^2$/sec and 3% windages are optimal for oil-spill simulations off the southeastern Mauritius coast.

**Keywords:** Wakashio, GNOME, winds, currents, stokes drift, oil spill budget

## 1. Introduction

Several oil spills accidents (major and minor oil spills) have occurred around the world in the past few decades (e.g. Exxon Valdez 1989, Gulf War 1991, Prestige 2002, Hebei Spirit 2007, Deepwater Horizon 2010, MV MSC Chitra 2010, Sanchi 2018). Some of these incidents have witnessed their impacts on the marine ecosystem (Peterson et al. 2003; Kujawinski et al. 2011; Kim et al. 2014; Boufadel et al. 2014; Xu et al. 2015; French-McCay et al. 2015; Yim et al. 2017; Nissanka and Yapa, 2017, Zhu et al. 2018; Yim et al. 2020). The oil spill incidents are also often evident in the Indian Ocean waters. For example, one of the major oil spill accidents on August 07, 2010, was a collision of the M.S.C. Chitra with MV Khalijia resulting in ≈ 800 tons of fuel oil off the Mumbai coast in the Arabian Peninsula Sea (Prasad et al. 2014). The *MT Dawn Kanchipuram* collided with *BW Maple* on January 28, 2017, resulting in ~200 tons of oil spill just two nautical miles away from the Chennai coast in the Bay of Bengal (Prasad et al. 2018). Both incidents have created massive damage to the marine environment. Oil spills in the marine environment would severely damage the marine ecosystem, mainly if they occurred near coastal and estuarine regions. In general, the sources of oil spills near coastal areas, harbours, and rivers are due to the grounding of ships, failures at oil rigs, cracked oil pipelines, and other factors (Chiu et al., 2018).

Remote Sensing technique played a significant role in oil spill detection, and the satellite SAR is widely used to monitor the oil spills in the marine environment (Garcia-Pineda et al., 2012; Caruso et al., 2013; Suresh et al. 2015; Zhao et al., 2015; Garcia-Pineda et al., 2017; Fingas and Brown, 2018; Suneel et al. 2019; De Dominicis et al., 2016; Pisano et al., 2016). Besides, these satellite observations have become very much helpful to validate several Lagrangian oil spill trajectory simulations due to the scarcity of in situ data (De Dominicis et al., 2016; Pisano et al., 2016, Prasad et al., 2018). Daneshgar Asl et al. (2017) have validated the hindcast model trajectories forced by the winds and currents (considering the deflection 20° and wind scaling coefficient 0.035) with the satellite observations and achieved good agreement between simulations and satellite observations. Tian et al. (2017) developed a new method to calibrate the Lagrangian model, and the calibrated model was further validated by the satellite Envisat ASAR images. Recently, Naz et al. (2021) studied four oil spill events that occurred during 2017-18 based on remote sensing observations and used them to validate the GNOME simulated trajectory predictions. Rajendran et al. (2021) have proved that SAR (Sentinel-1 and 2) sensors have the best ability to detect oil spills near the Mauritius region. In this study, the sentinel-1 Synthetic Aperture Radar (SAR) images have been considered to evaluate the GNOME model simulations.

Oil spill modelling is an effective tool for predicting its trajectory and identifying the coastlines that are likely to be affected. It is necessary for decision-makers during oil spill emergencies to initiate an effective clean-up operation immediately after the spill (Guo and Wang, 2009; Abascal et al., 2017a, b). Drifting of the oil slick on the sea surface is primarily due to the combined effects of wind stress, surface current, and the wave-induced stokes drift (Abascal et al. 2009, Spaulding, 2017). These forces are considered principal inputs for the simulation of a spill trajectory using a numerical modelling approach (Vethamony et al., 2007; Dominicis et al., 2016; Li et al., 2019; Pan, 2020; Barker et al. 2020). Kim et al. (2014a,b) studied the effects of wind drift factor on the drift of oil slick under strong tidal conditions at the western coastal area of Korea, considering the surface currents, wind speed and wind drift factor forcing parameters. However, the relative importance of these individual forces on spilled oil trajectory is regional dependent and can vary from incident to incident.

On July 25, 2020, the bulk carrier *MV Wakashio* ran grounded at Pointe- d'Esny, the southeastern coast of Mauritius, during its voyage from Singapore to Brazil. The ship carried ≈ 1.1 million gallons of low-Sulphur fuel oil, 63,000 gallons of diesel fuel, and 26,000 gallons of lube oils (NOAA, 2020). The Southeastern coast of Mauritius contains a wide range of sensitive coral, mangroves and fisheries. To protect this high sensitivity coastline and mitigate the spill's damage, the Government has attempted to pump off the oil from the tanker. Nevertheless, the persistent bad weather caused the rupture in the ship hull resulting in ≈1000 tons of fuel oil spilled (Latitude: -20.43 N, Longitude: 57.74 E) into the pristine waters of Mauritius Island, just 2 km away from the shore of Pointe d'Esney. The spill from the vessel was evident on August 06, 2020, and continued for a few days before the ship broke into two parts on August 15, 2020 (NOAA, 2020).

Therefore, the present study aimed to simulat the trajectories of *MV Wakashio* oil spill with different input forcing, primarily to unravel the dominant meteorology and oceanographic forces responsible for the deposited spill along the Southeastern Mauritius coast. These case studies are (i) Simulation of the model with only winds and currents influence, (ii) Simulation of the model with only winds influence, (iii) Simulation of the model with the only winds but different dispersion coefficient. The simulated trajectories were also validated with the Synthetic Aperture Radar (SAR) satellite imagery. Finally, the fate of oil spill has been estimated through oil budget analysis.

## 2. Study Area

The Republic of Mauritius is an Island located in the southwestern Indian Ocean basin (~20.10°S and 57.30°E) (Fig. 1), with 2.3 million $km^2$ of Exclusive Economic Zone (EEZ)

(Doorga et al. 2018). This Island has a coastline of ~ 200 km covered with 243 km$^2$ of lagoon area and 150 km fringing reefs in its vicinity (159 hard corals in 43 genera). The coastal fisheries are also confined to narrow coastal shelf (Lutz and Wills 1994). The coastal area consists of various habitats, including beaches, lagoons, mangroves, seagrass, corals (Daby, 2003, 2006). This study area is environmentally sensitive and protected under the international treaty for Ramsan conservation on wetlands (World Bank Group, 2017; Lewis 2020). The most densely maritime routes used for oil transportation in the Indian Ocean are situated close to this Island.

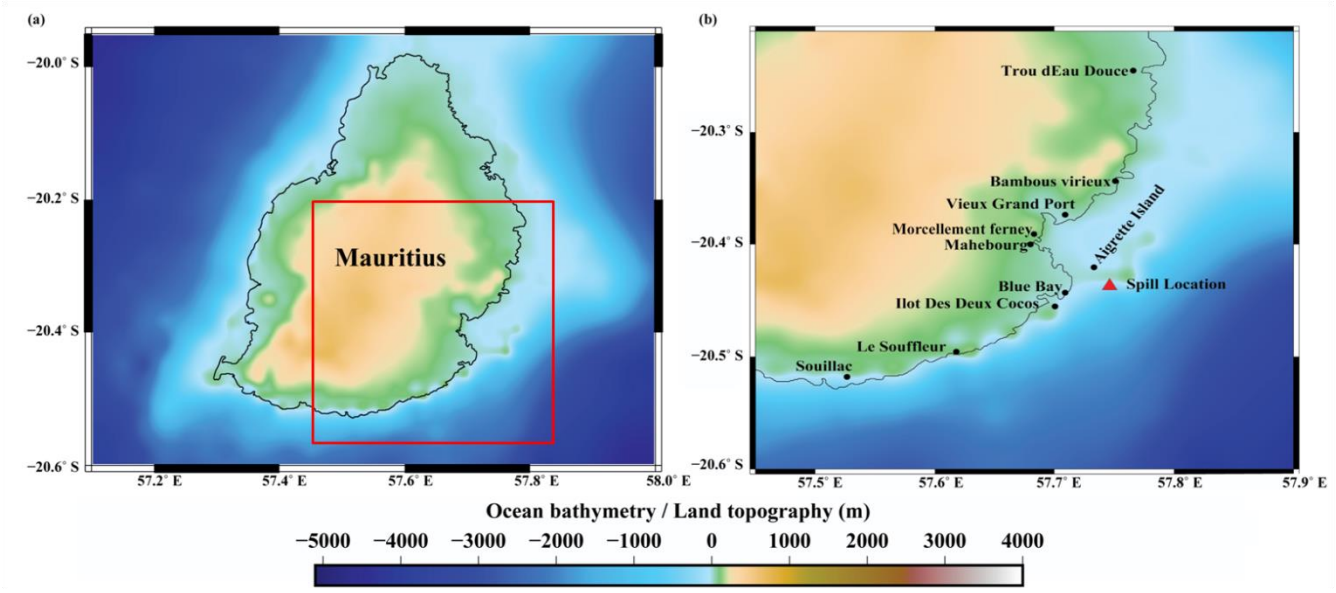


**Fig. 1**(a). Aerial **v**iew of Mauritius Island and its topography with the marked red colour square box is the study area, (b). The zoomed view of a red square marked in Fig. 1a.

Handling of the bunker fuel oils in Port Louis, the capital city of Mauritius Island, has been increasing due to the rise of shipping activities between Mauritius to Asia, Southern Africa, and South America. Increases in shipping activities are the potential risk for accidental oil spills (Singh et al., 2015). Therefore, this Island is highly vulnerable to the oil spills.

## 3. Data and Methodology

### *3.1. Data*

#### *3.1.1. Sentinel -1 Satellite imagery*

Several studies have been conducted to detect oil spills using sentinel-1 Synthetic Aperture Radar (SAR) imagery (Topouzelis et al. 2016, Suneel et al. 2019, and Naz et al., 2021). The high resolution (10×10 m) images of Sentinel-1 (1A and 1B), Level 1, Interferometric Width (IW), Grid (GRD) products were obtained from European Space Agency's Sentinels scientific data hub (https://scihub.esa.int/) for the days of 10, 16 and 22 August 2020; acquired at 01:37 hrs. These

images are used to validate the GNOME simulations. The discrimination of oil spills from look-alikes using single polarized (VV) sentinel-1 SAR imagery includes three steps viz. dark area detection, feature extraction and classification of oil/look-alike (Fingas and Brown, 2014; Migliaccio et al., 2015; Rajendran et al. 2021). The images were processed using Sentinel Application Platform (SNAP) programming, and the complete details of the image processing are given in Topouzelis et al. (2016), and Suneel et al. (2019).

### *3.1.2. Currents*

The measured currents during the simulation period are not available in this region. Therefore, HYCOM (Hybrid Coordinate Ocean Model) global model surface current velocities (http://hycom.org) were used. HYCOM is one of the most widely used models for operational oceanography, considering its potential to simulate the oceanic process with reliable ocean currents (Yao and Johns, 2010; Mezic et al., 2010; Mariano et al., 2011). It maintains significant advantages in stratified regions while allowing more vertical resolution near the surface and the shallow coastal area, hence providing a better representation of the upper ocean physics. Dauji et al. (2016) have evaluated the accuracy of the HYCOM simulated currents and found that excellent accuracy in the Indian Ocean. The global HYCOM provides currents with good spatial ($0.083^o$ x $0.083^o$) and temporal (3 hrs.) resolutions (Dauji and Deo, 2020) than any other available currents. Therefore, this study makes use of the freely available HYCOM currents.

Fig. 2 (a) and (c) show spatially averaged currents near the spill location. The current speed in our selected domain (20.228- 20.479 S and 57.636- 58.113 E) varies between 0.129-0.434 m/s, with an average speed of 0.284 m/s. The predominant current direction is towards the southwest near the spill location (Fig. 2a). However, the general circulation pattern in the South Equatorial Currents (SEC) intensifies at the surface, and it reaches up to 1400m depth whereas reduced when it's reaching the near shore. Besides, the reef canopy can also cause a reduction in current velocity (East et al. 2020) on the shelf.

### *3.1.3. Winds*

In addition to the currents, the surface winds are essential parameter for the GNOME model (Cheng et al. 2011). In this study, the hourly wind data were obtained from the reanalyzed wind fields of the European Centre for Medium Weather Range Forecast (ECMWF) Reanalysis (ERA5) (https://ecmwf.int) were used to force the GNOME model. Fig. 2 (d and e) shows a time series of wind speed and direction plotted from 06-24 August 2020. During this period, the moderate winds blowing from the southeast with the average speed of 6.1 m/s.

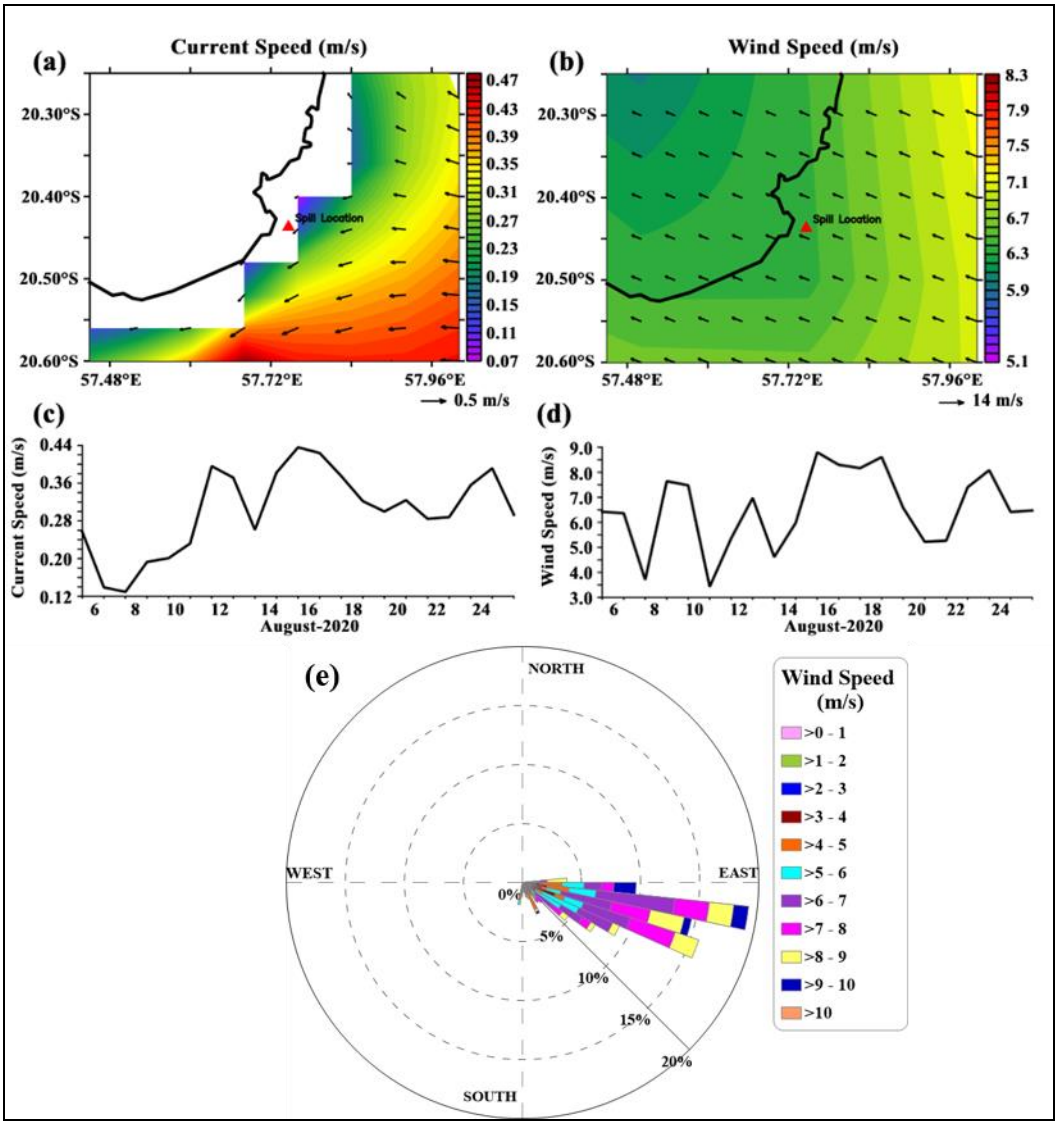


**Fig. 2.** Temporal averages of (a). HYCOM currents and (b) ERA5 winds in the study domain during 06-24 August 2020. (c) Spatially averaged current and (d) wind speed with time in the domain used for the oil spill simulation. (e) Wind Ross plot for the simulation period.

### *3.1.4. Stokes drift*

The transfer of momentum from atmosphere to ocean is primarily through the wind and wind-generated waves, which contribute to generating ocean surface currents (Mao and Heron, 2008). According to Stokes (1847), water particles have an additional movement in the direction of wave propagation, called Stokes Drift. The effect of wave-driven surface drift is mainly accounted by the Stokes Drift (Tang et al. 2007). Combined forces of wind, currents and waves (stokes drift) are the natural phenomenon that can primarily drift the oil spill both horizontally as well as vertically (Rohrs et al. 2018). Dominicis et al. (2016) studied the impact of currents, waves and winds on the multi-model approach. They found that the accuracy of oil spill model has been increased with the addition

of the Stokes drift when provided by wave. Therefore, accounting the influence of wind, currents and stokes drift is crucial to obtain the appropriate results on oil spill transport.

Stokes drift is dependent on wave field, which fluctuates by the smaller time scale within the area (Bennett and Mulligan, 2017; Montiel et al., 2018). The CMEMS (Copernicus Marine Environmental Monitoring Service) provides the stokes drift data for daily and monthly mean velocities (Fig. 3). The CMEMS database produces the information using the Meteo-France WAve Model (MFWAM) by Meteo-France global wave system. Here, the wave products are the integrated parameters computed from the total wave spectrum (significant wave height, period, direction, Stokes drift) and the wind wave, the primary and secondary swell wave. The spatial resolution for the model domain is 1/12° (approx. 8 km) with the regular grid of 4320 x 2041.

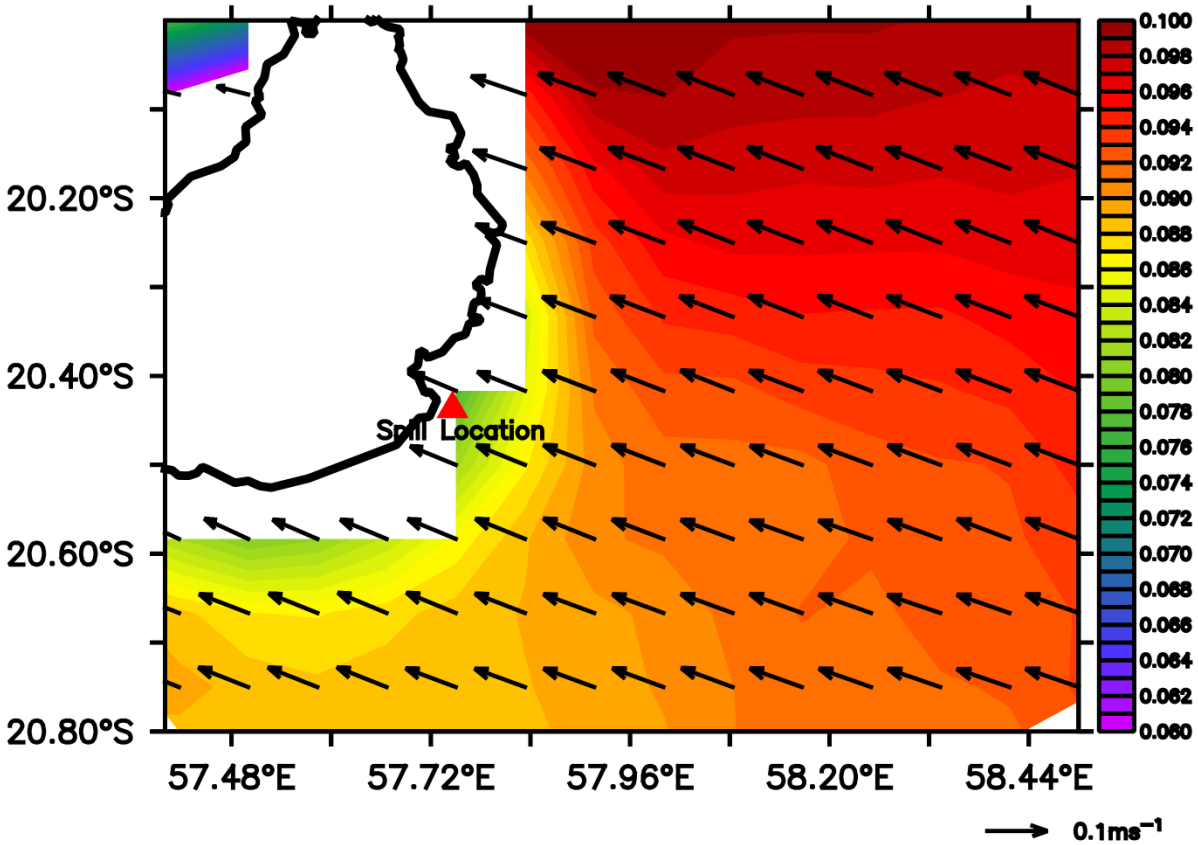


**Fig. 3.** The temporal average of Stokes drifts in the study area during 6-24 August 2020.

### *3.2. Methodology*

In this study, we used the diagnostic mode of the GNOME model driven by ocean surface winds and currents (Beegle-Krause, 2003, 2005). The GNOME oil spill model developed by the Hazardous Materials Response Division (HAZMAT) of the National Oceanic and Atmospheric Administration Office of Response and Restoration (NOAA OR&R) (Duran oet al. 2018). This 2D Eulerian/Lagrangian model has been used widely for the marine, coastal and riverine regions

(Farzingohar et al. 2011; Cheng et al. 2011) to track the possible oil slick movement (Zelenke et al. 2012, ITOPF 2019). The movement of oil caused by the wind is known as windage, which is typically 3% of the wind speed on the surface. Reed et al. (1994) suggested a 3.5% wind factor gives a good simulation while using the wind without wave breaking. Abascal et al. (2009) experimented with the oil spill drift by using two different wind drag coefficients (0.025, 0.044); and found that both the simulations have predicted the same place of stranding, but a difference of 20 km was observed between those simulations. Several works of literature reported the mean wind factor varies from 3-3.5%. Based on the analytical derivation, observations and overflight reports, the GNOME model recommends 1%-4% as the default wind factor (Stolzenbach et al. 1997; GNOME, 2012).

The performance of the GNOME oil spill model is depending on the model configuration including the input forcing. Therefore an attempt has been made to simulate the model with different windage factors in the range minimum to maximum, such as 0%, 3%, 4% and 6%, to account the effect of wind drag on the oil slick movement (Figure not shown). The simulation results showed that the 0% windage resulted very low beaching, and the 6% windage resulted very high beaching in line with Boufadel et al. (2014). Therefore, we considered 3% wind factor may be optimal for the simulation, which was also used by Prasad et al. (2018). Diffusion, i.e. random spreading, is also included in this model by a simple random walk with a square unit probability. The random walk is based on the model's diffusion value, which represents the horizontal eddy diffusivity. The Stochastic diffusion processes in GNOME can be applied using the Cartesian coordinates diffusion equation (GNOME, 2012).

$$\frac{\partial C}{\partial t} = D_x * \frac{\partial^2 C}{\partial x^2} + D_y * \frac{\partial^2 C}{\partial y^2} \qquad \textbf{Equation 1}$$

C is the concentration of a material, and D$x$ and D$y$ is the scalar diffusion coefficients in the x and y directions. So, diffusion can be simulated with a random walk with any distribution. The resulting diffusion coefficient is one half the variance of the distribution of each step divided by the time-step.

$$D_x = \frac{1}{2} * \frac{\sigma_x^2}{\Delta t} \qquad \textbf{Equation 2}$$

GNOME compute a ($\Delta x$, $\Delta y$) from the input diffusion coefficient D, and at each diffusion time-step, *dx* and *dy* are chosen randomly from a uniform distribution (of floating-point numbers) between -1 and 1 such that $-\Delta x \leq dx \leq \Delta x$, $-\Delta y \leq dy \leq \Delta y$, and $\Delta x = \Delta y$. The value of horizontal diffusion varies from 1000 to 100,000 $cm^2/s^{-1}$ (low to high), with the default value of 100,000 $cm^2/s^{-1}$. Thus, the simulated oil diffusion area also varies by magnitude. GNOME recommends a default value of 100,000 $cm^2/s^{-1}$, widely used for spilled oil movement (Zelenke et al., 2012; Prasad et al., 2018).

Therefore, the diffusion of 100,000 $cm^2/s^{-1}$ is used in the present study for the model simulations. However, to ensure the role of diffusion on the spreading area of floating oil and beached oil and hence to depict the probabilistic minimum and maximum contaminated site, we choose two different coefficient values considering 20,000 $cm^2/s^{-1}$ as low and 100,000 $cm^2/s^{-1}$ as default values for the simulations. Although both values yield more or less similar results, the default value of 100,000 $cm^2/s^{-1}$ delivers relatively better results (Table 1).

GNOME also uses a simplistic 3-phase evaporation algorithm (Equation 3) where the pollutant is treated as a three-component substance with independent half-lives (Boehm et al. 1982).

$$X_{prob} = \frac{P_1 * \left(2^{\frac{-t_i}{H_1}} - 2^{\frac{t_{i-1}-2*t_i}{H_1}}\right) + P_2 * \left(2^{\frac{-t_i}{H_2}} - 2^{\frac{t_{i-1}-2*t_i}{H_2}}\right) + P_3 * \left(2^{\frac{-t_i}{H_3}} - 2^{\frac{t_{i-1}-2*t_i}{H_3}}\right)}{P_1 * 2^{\frac{-t_i}{H_1}} + P_2 * 2^{\frac{-t_i}{H_2}} + P_3 * 2^{\frac{-t_i}{H_3}}} \quad \textbf{Equation 3}$$

T and t1 are the time elapsed (age; in hours) at time-step i and the previous time-step i-1. $H_1$, $H_2$, and $H_3$ are the half-lives of each constituent (in hours), and $P_1$, $P_2$, and $P_3$ are the percentages of each constituent (as decimals).

GNOME has an option for refloating or resuspension of oil determined by refloating half-life, which is defined as the number of hours in which the beached oil removed by (i) the offshore wind or diffusion transport (Zelenke et al. 2012; Amir-Heidari et al. 2019) and (ii) same or higher the sea level. The spilled oil may move towards the wind direction to reach the coast, and they may again return to the water to pollute the nearshore region (Amir-Heidari et al., 2019). Though the predominant winds are southeasterlies, they had varied between easterlies to southerlies (Fig. 2e), and whenever high tide occurs, the sea level rises and may favour the refloating of oil. Therefore, to include a rising tide effect, we considered the GNOME recommended default refloat half-life in this study, which is 1 hour. Jones et al. (2016) have considered 12 hours refloat half-life for the shelf model to sandy beaches.

The *MV Wakashio* oil spill trajectories have been simulated using currents and winds (case-1) are the driving forces and the diffusion coefficient of 100,000 $cm^2$/sec. Initially, the spill quantity of 1000 tons was released during 06-16 August 2020, followed by the release of another 50 tons during 16-22 August 2020 at the location where the ship *MV Wakashio* has grounded (Latitude: -20.43 N, Longitude: 57.74 E). Therefore, the total simulation period was 18 days.

**Table 1. GNOME model setting for the three cases of oil spill simulations**.

| Case study | Forcing | Diffusion ($cm^2/s$) | Spill location | Simulation period | Spill Quantity(tons) |
|---|---|---|---|---|---|
| 1 | 3 hourly Current + Hourly wind | 100,000 | 20.438 S 57.745 E | 06-24 August 2020 | 1050 |
| 2 | Hourly wind | 100,000 | 20.438 S 57.745 E | 06-24 August 2020 | 1050 |
| 3 | Hourly wind | 20,000 | 20.438 S 57.745 E | 06-24August 2020 | 1050 |

The location of the oil spill was identified from the Synthetic Aperture Radar (SAR) imagery. The volume of spill oil has denoted as a 'splot' representing the portion of spilled oil in the actual scenario. An amount of 1000 tons of fuel oil (10000 splots) have been released continuously between 06-August-2020 06:30 am to 16-August-2020, 23:00. The ship had broken into two parts before it sank on August 15, and there were around 50 tons of oil remaining (Press Report: CBS News, 2020a). Therefore, additional 50 tons of fuel oil (1000 splots) have been released from August 16, 2020, 23:30 to August 22, 2020, 23:00 in the simulation. These splots represent the average amount of oil released to the water surface daily until the leak ends.

## 4. Results and discussion

### *4.1. Case 1: Simulation of oil spill trajectory with current and wind*

Snapshots of the simulation taken after the days of 1$^{st}$, 2$^{nd}$, 4$^{th}$, 8$^{th}$, 16$^{th}$, and 22$^{nd}$ were illustrated in Fig. 4. The black and red colour dots in Fig. 4 represent Best Guess Solution (BGS) and Minimum Regret Solution (MRS), respectively. Fig. 4 depicts that initially, the floating oil has drifted westward and reached the southeast Mauritius coast at Pointe d'Esny in 2 hours 30 minutes, and until the first 6 hours, it had continued to move in the same direction and reached the shore. After 6 hours, some portion of the oil started drifting towards the northwest direction (NW). The model result illustrated the beaching of the oil particles at Blue Bay and Aigrettes Island on August 06 at 17:00 hours. After that, part of the oil particles moved towards the NW direction; however, ≈12 tons (at time of 17:00 hours) of oil beached along the coastal stretch of Pointe d'Esny. The current speed was constantly reducing from August 06 to August 08 2020 (Fig. 2). As also evidenced in Fig. 2 (e), winds could have played a significant role in drifting the spill westward during the study period.

The simulation after four days depicts that most of the oil particles were drifted only in the SW direction for the entire simulation period. As shown in Fig. 4, the oil is primarily drifted westward to northwestward direction during the early days of simulation, after that drifted southwestward

direction. These simulation results are not reasonably matching with the SAR imagery (discussed in later sections). Therefore, the simulation has been performed, considering only the wind forcing as case study 2.

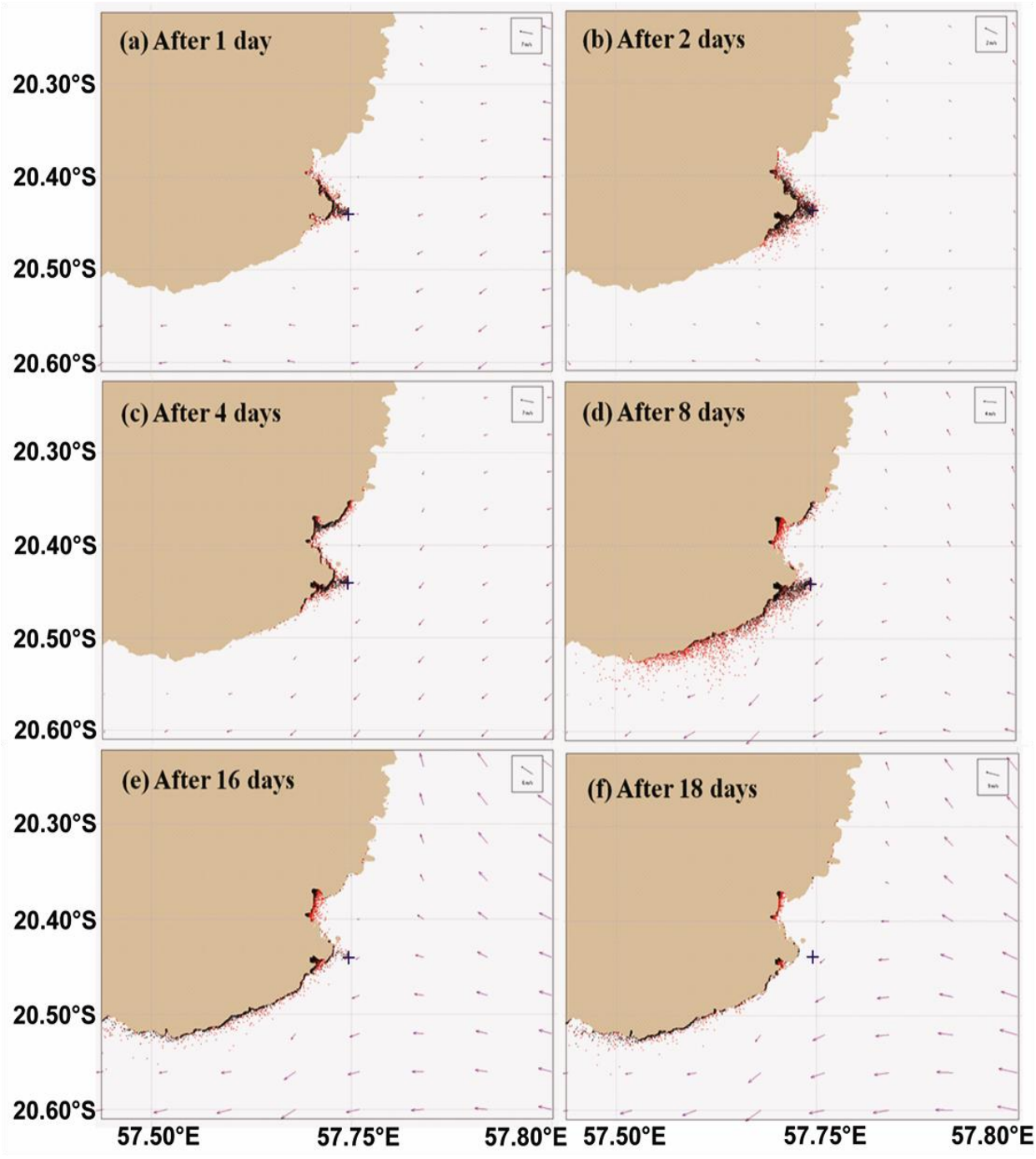


**Fig. 4.** Simulation of oil spill with both wind and current forcing and default diffusion of 100000 $cm^2$/sec. Panels (a), (b), (c), (d), (e) and (f) represents the snapshots of the simulations taken at 1, 2, 4, 8, 16 and 18 days respectively.

### *4.2. Case 2: Simulation of oil spill trajectory with only wind*

In this case, we considered wind as the only forcing parameter for the oil spill simulation. Fig. 5 depicts the drift of the spill was predominantly northwest during the simulation period (06-24 August 2020). Initially, the oil particles were drifted westward and started beaching along the coast of Pointe d'Esny, which is ~2 km away from the spill location. According to the model simulation, ~0.2 tons of oil was beached along the Pointe d'Esny (-20.434 S, 57.727 E) within 3 hours 15 minutes from the spill time. The spreading has extended ~0.8 km along the Pointe d'Esny (centre part- northern part) within 5 hours and 30 minutes indicates that the oil spill severely impacted the sandy beaches along the coast of Pointe d'Esny. Although most of the oil patches drifted towards the northwestward direction, the Aigrettes Island located in between was also affected after August 08 2020, at 12:15 pm. The prevailing southeasterly solid winds advected the oil particles northwestward along the coastline of Mahaburg. According to the GNOME simulation, after initial 24 hours, about 41 tons of oil beached along ~7 km from Pointe d'Esny to reef entrance towards Vieux Grand Port. Overall, coastal regions such as Pointe d'Esny, Mahaburg, Morcelement Ferney, Grand Port, and Coral residence were highly impacted by the spill. The local news report also confirms that clean up activities have been initiated in these coastal areas (Press Report: Scientific American; Press Report: news18).

As evident in Fig. 5(a), the large amount of beached oil is continued to be stranded along the shore, but the refloating of oil back to the sea is comparatively less. The northwestward drift pattern was observed for the first 48 hours (6-7 Aug 2020). After that, oil has moved northward (from August 08, 11:30) under the wind speed of 5 m/s. During this period, 80% of the beached oil also refloated with fresh floating oil and settled along the coast of south Vieux Grand Port to Bambous Virieux (~8 km). Allshouse et al. (2017) have reported these complex advective phenomena of beaching/refloating that depend on various shoreline types, as well as detailed windage analyses.

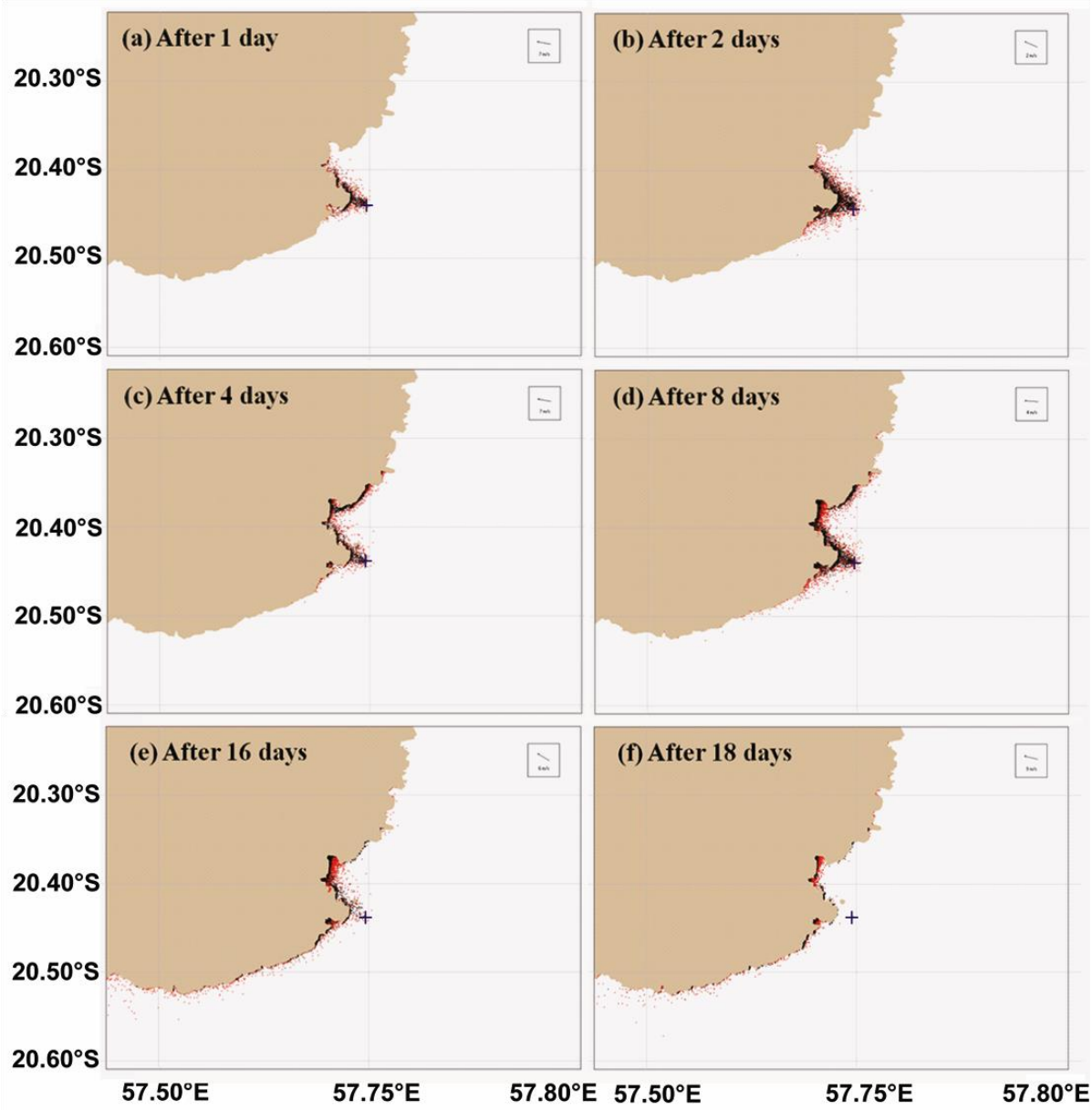


**Fig. 5.** Simulation of oil spill with only wind forcing and default diffusion of 100,000 $cm^2$/sec. Panels (a), (b), (c), (d), (e) and (f) represents the snapshots of the simulations taken at 1, 2, 4, 8, 16 and 18 days respectively.

Time evaluation of spilled oil trajectory for 18 days study period follows the wind pattern, predominantly moves northwestward. The quasi-permanent high-pressure system in the Indian Ocean generates constant southeasterly winds and waves throughout the year, with wind speeds vary from 5 m/s to 25 m/s from June to September (Dhunny et al., 2015). Wind speed varies between 1.4 m/s and 10.5 m/s with an average of 6.1 m/s. They directed between 85.7° to 190.4° with an average of 115.1° in the present domain (Fig. 2e). These strong southeasterly winds that prevailed on the east coast of Mauritius must have contributed majorly to the movement of oil towards the northwest direction. Relatively, fewer particles were drifted southwestward up to Souillac coastal area. Fig. 5

clearly shows that floating MRS is more than the floating/beached BGS along the southwest coastal region, which significantly high in case study-1, where the simulation was performed with both wind and current forcing. These results indicate that winds have played a significant role in drifting the *MV Wakashio* oil spill towards the Mauritius coast. Maslo et al. (2014) found that the wind effect decreases the velocity of the slick by pushing it towards the shore. Pradhan et al. (2020) studied the hypothetical oil spill trajectory off Odisha coast, Bay of Bengal using the GNOME model; their result showed that wind speed and direction have a significant role in the oil spill movement.

The validation of the model simulations with current and wind; and the wind was performed comparing with the available SAR imagery. The images obtained on the days of 10, 16, and 22 August 2020 (at 01:37) were compared with snapshots of the GNOME model captured at 01:30 am. Good agreement between the GNOME simulation (only with the wind) and the SAR imagery was observed, as showed in Fig. 6 (b, d, and f). It shows that the oil particles were primarily drifted towards the northwest as observed in SAR imagery, and there was also a southwestward drift with BGS and MRS. BGS is comparatively less than MRS, which is shown in Figs 2 and 4. It may be noted that according to the SAR images available on $10^{th}$, $16^{th}$, and $22^{nd}$ August 2020, there was no clue of oil slicks towards south or southwest from the spill location. However, the simulation on 16 and 22 August (Fig. 6d, f) indicates a significant drift of oil particles towards the southwest.

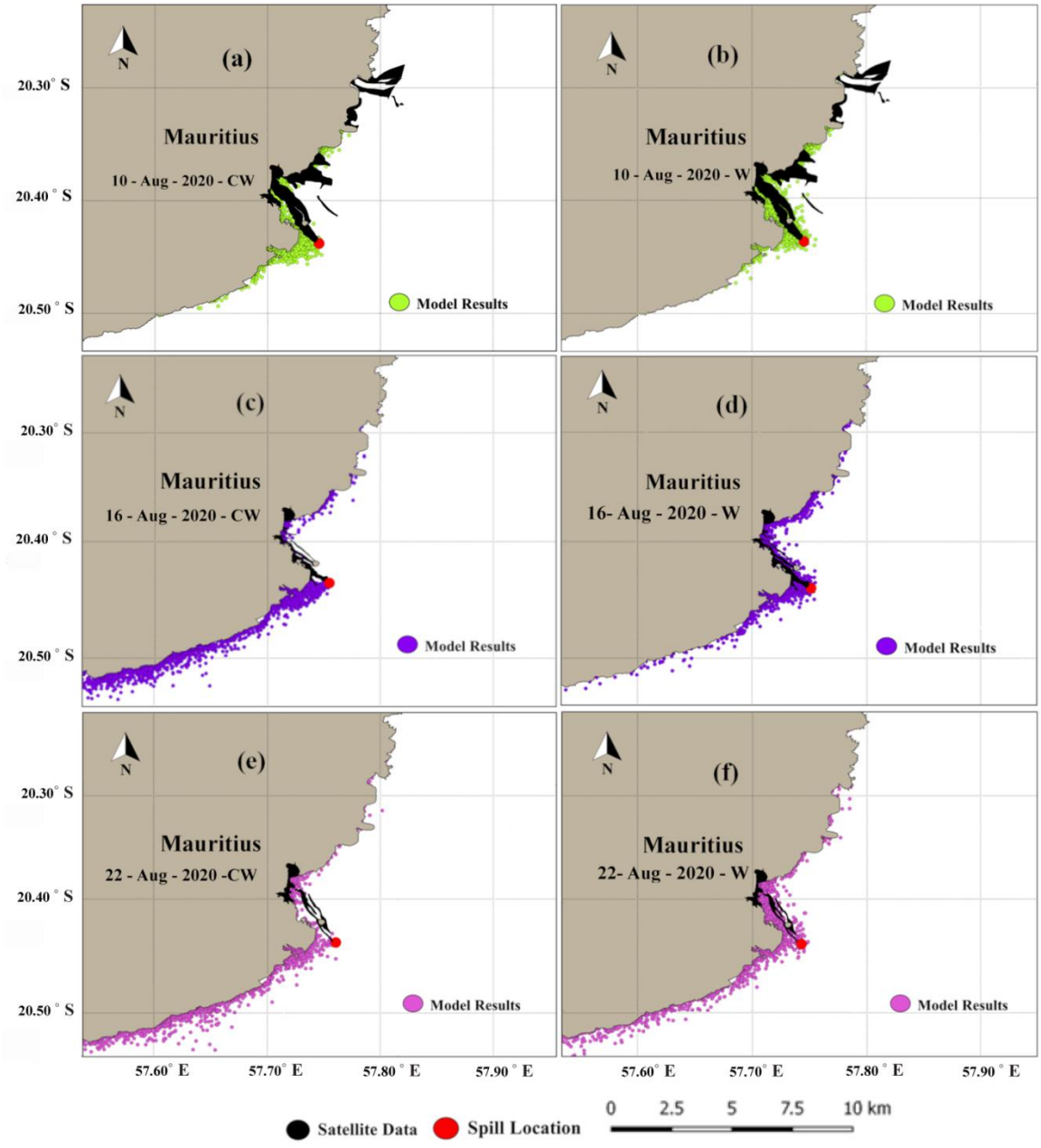


**Fig. 6.** Model simulations overlaid with SAR images. Figs (a), (c) and (e) are the simulations performed with wind and current. Figs (b), (d), and (f) are the simulations performed with only wind considering 100,000 $cm^2$/sec diffusions for all the cases.

There could be multiple reasons for this erroneous southwestward drifting of oil. (i) GNOME does not consider tides: Tides may play a significant role in drifting the oil particles towards the shore/coast during the high/low tide (Lee et al. 2020; Kim et al. 2013). (ii) Errors in hydrodynamics used in the GNOME: The HYCOM currents used in this study are of 1/12 ° resolution (9.5 km), are one limitation to the very nearshore region studies, and a coarser bathymetry may also lead to errors in the hydrodynamic simulations (Barker et al. 2020). Hence such errors may not depict the realistic

currents in the nearshore region. (iii). GNOME does not consider the actual barriers (booms etc.): The proximity of the containment activities such as booms, handmade natural floating material (dried sugarcane leaf or straw), and crisscrossed fibres were actually deployed in the near sensitive regions, including the seaward entrance of Blue Bay Marine Park (Press Report: The India express, 2020). These effects are not included in the model simulation. Thus, the non-inclusion of tides and booms effect in the GNOME, and the limitations of HYCOM currents, could have caused the southwestward drift of spill in the GNOME simulations.

The other important force that can influence the surface oil spill drift is Stokes Drift. The Stokes Drift has been considered in numerous studies particularly to simulate the drift, deformation and prediction of oil slicks trajectories (Christensen and Terrile 2009, Daniel et al. 2003; Abascal et al. 2009; Azevedo et al. 2009). Unfortunately, the GNOME could not include the influence of Stokes Drift. Therefore, in this study we separately analysed the influence of Stokes Drift. The Fig. 3 illustrates that the spatially averaged Stokes drift is primarily northwestward during the study period, similar to the prevailed wind pattern (Fig. 2b). Therefore, based on Fig. 2b, and Fig. 3 it evident that the stokes drift might have also contributed to the predominant northwestward drift of the spill in addition to the winds. Tuomi et al. (2018) have shown that the direction of Stokes drift mostly followed the wind direction and found to be very similar although the magnitudes of the wind drift are found to be larger. Therefore, it is evident that the predominant northwestward drift of oil spill is due to the cumulative forcing of winds and stokes drift.

### *4.3. Case- 3: Simulation of oil spill trajectory with the only wind but different diffusion*

In this case, the simulation was performed with the only wind and diffusion coefficient of 20,000 $cm^2/s$ to understand the influence of diffusion on slick spreading. SAR imagery was used to validate the simulations. Fig. 7 illustrates the validation of case-2 and case-3 model results with SAR observations. The Fig depicts that both the simulation performed with the diffusion of 20,000 $cm^2/s$ and 100,000 $cm^2/s$ are similar. Still, the careful examination suggests that simulation of 100,000 $cm^2/s$ are in better agreement with SAR in terms of spreading over the larger area of the image (Fig. 7(b), (d), and (f)). Therefore, our results also suggest the default diffusion value of 100,000 $cm^2/s$ yields comparatively good results in supporting the previous studies (Zelenke et al. 2012 and Prasad et al. 2018).

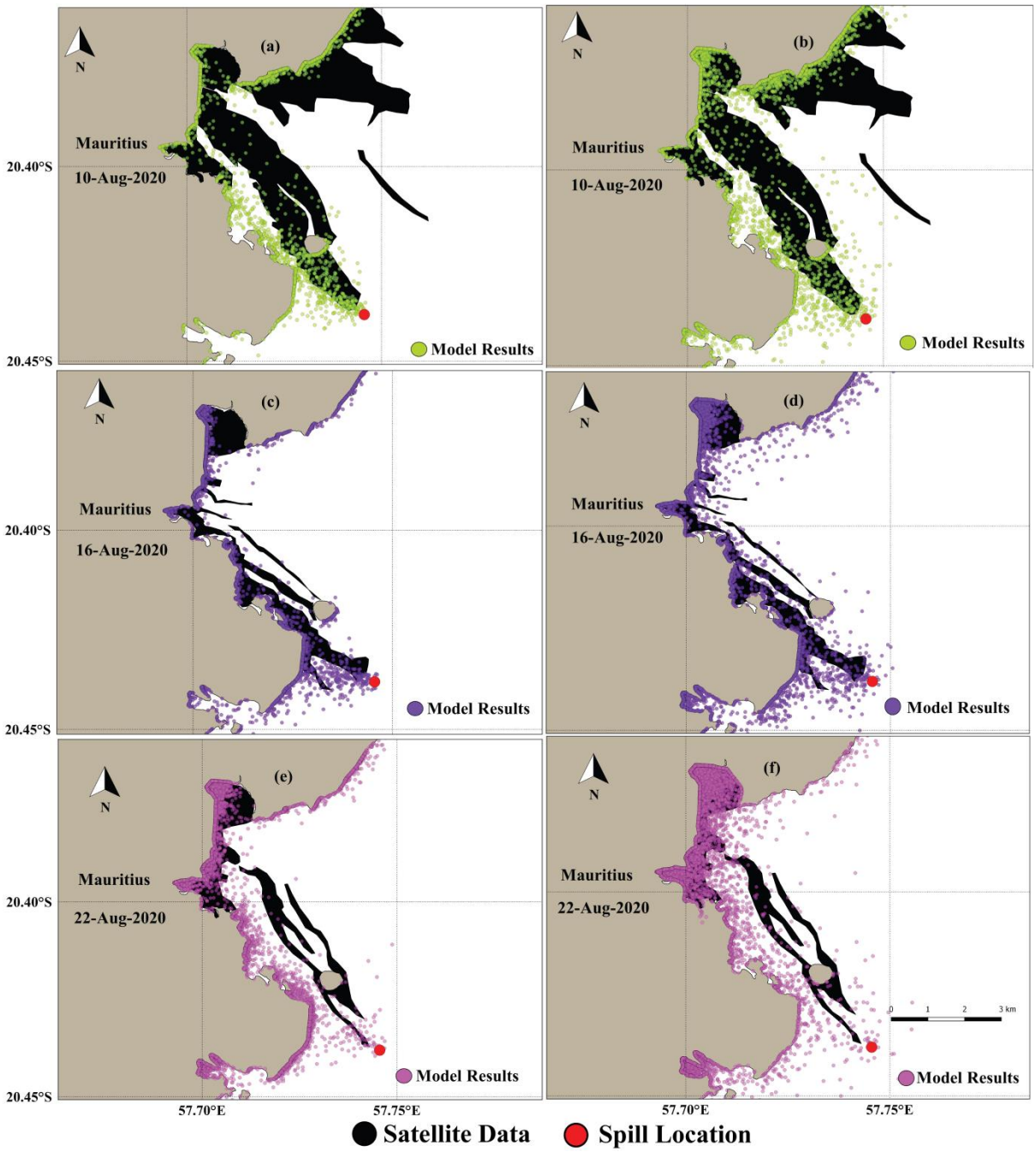


**Fig. 7.** Comparison of case-3 (only wind but different diffusion coefficients) and case-2 (only wind with default diffusion coefficient) simulations with SAR imagery. Fig. (a), (c) and (e) are the simulations performed with 20,000 $cm/s^2$ overlaid by the respective SAR imagery (case-3). Similarly, Fig. (b), (d) and (f) are the simulations performed with 100,000 $cm/s^2$(case-2) overlaid by the respective SAR imagery.

### *4.4. Mass balance of the spilled oil*

GNOME can estimate the mass balance of the spilled oil during its exposure to the surface water. Assessment of approximate quantities of the floating oil, beached oil, evaporated, and dispersed oil have been performed to understand their impact on the marine environments. Fig. 8a and b depict the simulated oil budget during the study period. The evaporation process is activated within 1 hour 30

minutes after the simulation has started, and it increased gradually till the end of the 1000-ton spill (August 16). After that, no changes have occurred, and it continued to be more or less the same till the end of the simulation (Fig. 8a). During the initial time of simulation (06-08-2020; 08:00hrs), ~0.1 ton of oil were evaporated out of 5 tons released, but on the whole, 344 tons (out of 1000 tons) and 15.3 tons (out of 50 tons) of oil is evaporated (Fig. 8a and b). The relationship between beached oil and floating oil is evident. When the amount of beached oil has increased, then the floating oil has decreased, indicating a significant portion of the oil is getting beached. The estimated amount of beached oil is about 584 and 30.5 tons out of 1000 tons and 50 tons, respectively, with the cumulative amount of 614.5 tons (Fig. 8a and b). This amount of spill could surely make severe impacts on the marine environment. The biodiversity of coral reefs, mangroves, fisheries, and seagrass will be highly under threat. Almost 39 dolphins, crabs, sea birds, and starfish have been found dead and washed ashore after this worst spill. Based on the model result, it is evident that the beached oil may have severe impacts on the River Des Creoles. The local report also confirmed through clean up activities in the mangroves region of the River Des Creoles (Press Report: NYTimes; Press Report: cbsnews, 2020b). Model results showed that around 75.3 tons of oil remained floating on the water (on 24-08-2020 06:30) and might have reached the coast in subsequent time (after 18 days from the spill). Therefore, effective clean up activity and continuous monitoring of the marine ecosystem shall have to be continued further.

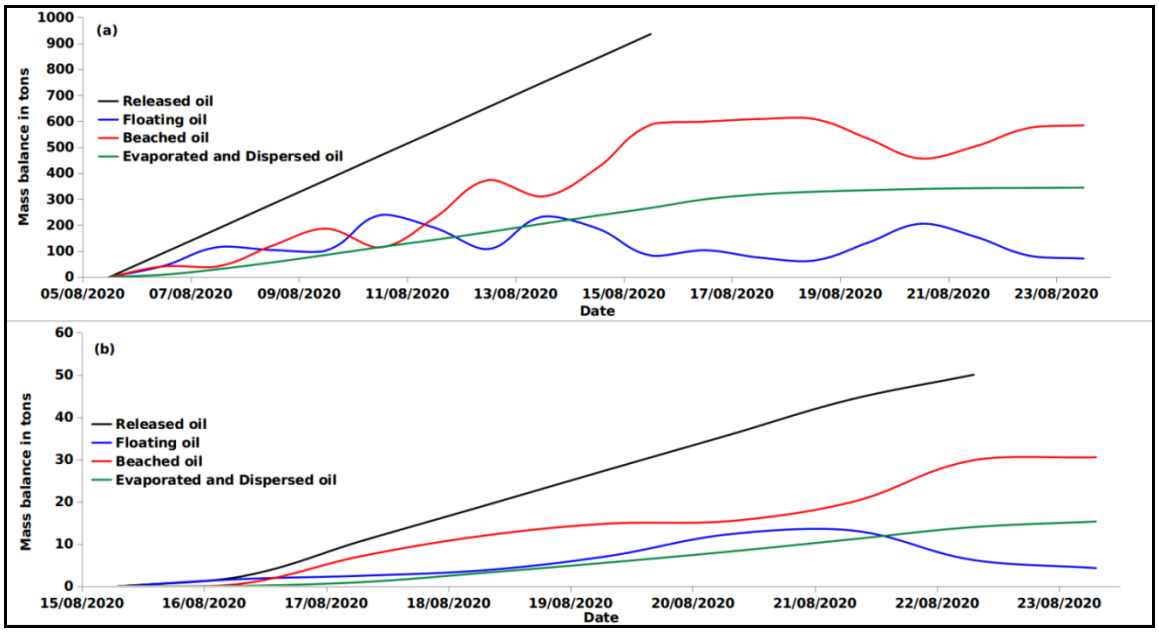


**Fig. 8.** GNOME derived Mass balance (a) during the period 06-16 August 2020 represents the scenario of 1000 tons, and (b) during the period 16-22 August 2020 represents the scenario of 50 tons spill.

## 5. Conclusion

This study investigated the fate of the *MV Wakashio* oil spill in the Indian Ocean Island of Mauritius by using the well-known GNOME model. Its simulated trajectories were also validated with SAR imagery. Thus, an attempt has been made to identify the meteorology and oceanographic forces responsible for the observed drift of spill during this episodic event of the Wakashio oil spill. Simulations were performed as three cases considering the influence of (i) wind and current, (ii) only wind (iii) only wind but with different diffusion. The simulation model results are in good agreement with SAR data when performed only with wind, indicating that wind played a major role in drifting the *MV Wakashio* oil spill towards the coast. The depicted stokes drift also suggests its additional contribution to the drift of spill towards the northwest. Therefore, most of the oil particles that drifted northwestward matching with the SAR imagery were due to the cumulative effect of wind and stokes drift pattern. Our analyses also revealed that the diffusion coefficient of 100,000 $cm^2$/sec and 3% windages are optimal for the oil-spill simulations off the Mauritius coast. Based on the oil budget analysis, it is estimated that ~ 615 tons of oil have been beached along a 15 km long coastline between Pointe d'Esny to Vieux Grand Port, including Mahaburg. Although there are no in situ observations to validate the same, according to the National Crisis Committee report, ~1122 tons of contaminated liquid waste (oil mixed with seawater) and ~ 792 tons of contaminated solid on the shore has been carted away (NCC, 2020). The one limitation of the present study is that the tides and waves were not considered, which could undoubtedly improve the model performance. Further investigation should be needed to highlight the environmental and ecological impacts.

## Acknowledgements

Authors would like to thank the Director, CSIR-National Institute of Oceanography (CSIR-NIO), Goa, for providing facilities to carry out the study. We also acknowledge the Sentinel Scientific Data Hub, HYCOM and ECMWF-ERA5 for free access to data. We thank the Emergency Response Division of the National Oceanic and Atmospheric Administration of the United States for providing the GNOME. The comments from the anonymous reviewers were helpful in improving the quality of the manuscript. This is CSIR-NIO contribution number XXXX.

## References


Abascal, A.J., Castanedo, S., Mendez, F.J., Medina, R., Losada, I.J., 2009. Calibration of a Lagrangian transport model using drifting buoys deployed during the prestige oil spill. J. Coast. Res., 251, pp. 80-90.

Abascal, A.J., Castanedo, S., Nunez, P., Mellor, A., Clements, A., Perez, B., Cardenas, M., Chiri, H., Medina**,** R., 2017a. A high-resolution operational forecast system for oil spill response in Belfast Lough. Mar. Pollut. Bull., 114, pp. 302-314.

Abascal, A.J., Sanchez, J., Chiri, H., Ferrer, M.I., Cárdenas, M., Gallego, A., Castanedo, S., Medina, R., Alonso-Martirena, A., Berx, B,.Turrell, W.R., Hughes, S.L., 2017b. Operational oil spill trajectory modelling using HF radar currents: a northwest European continental shelf case study. Mar. Pollut. Bull., 119, pp. 336-350.

Allshouse, M.R., Ivey, G.N., Lowe, R.J., Jones, N.L., Beegle-Krause, C. J., Xu, J., Peacock, T., 2017. "Impact of windage on ocean surface Lagrangian coherent structures," Environmental Fluid Mechanics 17, 473–483.

Amir-Heidari, A., Arneborg, L., Lindgren, J.F., Lindhe, A., Rosen, L., Raie, M., Axell, L., Hassellov, I.M., 2019. A state-of-the-art model for spatial and stochastic oil spill risk assessment: A case study of oil spill from a shipwreck. Environmental International 126, 309-320.

Azevedo, A., Oliveira, A., Fortunato, A. and Bertin, X. 2009. Application of an Eulerian-Lagrangian oil spill modeling system to the Prestige accident: trajectory analysis. Journal of Coastal Research, SI 56 (Proceedings of the 10th International Coastal Symposium), 777 – 781. Lisbon, Portugal, ISSN 0749-0258.

Azevedo, A., Oliveira, A., Fortunato, A., Bertin, X., 2009. Application of an Eulerian-Lagrangian oil spill modeling system to the Prestige accident: trajectory analysis. Journal of Coastal Research, SI 56 (Proceedings of the 10th International Coastal Symposium), 777 – 781. Lisbon, Portugal, ISSN 0749-0258.

Barker, C.H.,Kourafalou, V.H., Beegle-Krause, C.,Boufadel, M., Bourassa, M.A.,Buschang, S.G.,Androulidakis, Y.,Chassignet, E.P., Dagestad, K.F.,Danmeier, D.G.,Dissanayake, A.L., Galt, J.A., Jacobs, G.,Marcotte, G., Ozgokmen, T.,Pinardi, N., Schiller, R.V.,Socolofsky, S.A., Thrift-Viveros, D.,Zelenke, B., Zhang, A., Zheng, Y., 2020. Progress in Operational Modeling in Support of Oil Spill Response. J. Mar. Sci. Eng., 8 (9), 668. https://doi.org/10.3390/jmse8090668.

Beegle-Krause, C.J., 2003. Advantages of Separating the Circulation Model and Trajectory Model: GNOME Trajectory Model Used with outside Circulation Models, Proceedings of the Twenty-sixth AMOP Technical Seminar, Environment Canada, Ottawa, ON, pp. 825-840.

Beegle-Krause, C. J., 2005. Combining modelling with response in potential deep well blowout: Lessons learned from Thunder Horse. International Oil Spill Conference Proceedings 2005, pp.1-4.

Bennett, V. C., Mulligan, R. P., 2017. Evaluation of surface wind fields for prediction of directional ocean wave spectra during hurricane sandy. Coastal Engineering, 125, 1–15.

Boehm, P.D., Fiest, D.L., Mackay, D., Paterson, S., 1982. Physical chemical weathering of petroleum hydrocarbons from the Ixtoc I blowout: chemical measurements and a weathering model. Environment Science and Technology, 16, 498-505.

Boufadel, M.C., Abdollahi-Nasab, A., Geng, X., Galt, J., Torlapati, J., 2014. Simulation of the Landfall of the Deepwater Horizon Oil on the Shorelines of the Gulf of Mexico. *Environ. Sci. Technol.* 48(16), 9496–9505.

Caruso, M.J., Migliaccio, M., Hargrove, J.T., Garcia-Pineda, O., Graber, H.C., 2013. Oil spills and slicks imaged by synthetic aperture radar. Oceanography 26 (2), 112–123.

Cheng, Y., Li, X., Xu, Q., Garcia-Pineda, O., Andersen, O.B., Pichel, W.G., 2011. SAR observation and model tracking of an oil spill event in coastal waters. Mar. Pollut. Bull., 62 (2), pp. 350-363.

Chiu, C, M., Huang, C, J., Wu, L, C., Zhan, Y, J., Chuang, L, Z, H, Fan, Y., Yu, H, C., 2018. Forecasting of oil-spill trajectories by using SCHISM and X-band radar. Mar. Pollut. Bull. 137, 566–581.

Christensen, K.H., Terrile, E., 2009. Drift and deformation of oil slicks due to surface waves. Journal of Fluid Mechanics 620, pp. 313-332.

Daby, D., 2003. Effects of seagrass bed removal for tourism purposes in a Mauritianbay. Environ. Pollut. 125, 313e324. https://doi.org/10.1016/S0269-7491(03)00125-8.

Daby, D., 2006. Current patterns and the distribution of benthic habitats in a coastal lagoon of Mauritius. Hydrobiologia 556, 47e60.https://doi.org/10.1007/s10750-005-0593-7.

Daneshgar Asl, S., Dmitry S. Dukhovskoy, Mark Bourassa, Ian R. MacDonald., 2017. Hindcastmodeling of oil slick persistence from natural seeps. Remote Sensing of Environment 189, 96–107.

Daniel, P., Marty, F., Josse, P., Skandrani, C., Benshila, R., 2003. "Improvement of drift calculation in Mothy operational oil spill prediction system", In International Oil Spill Conference. April, 2003: 1067-1072, American Petroleum Institute, 2003.

Dauji, S., Deo, M.C., 2020. Improving numerical current prediction with Model Tree. Indian Journal of Geo Marine Sciences, 49 (08), 1350-1358.

Dauji, S., Deo, M.C., Joseph, S., Bhargava, K., 2016. Environ. Syst. Res., 5(4), DOI 10.1186/s40068-016-0057-2.

De Dominicis, M.,Bruciaferri, D., Gerin, R.,Pinardi, N.,Poulain, P.M.,Garreau, P.,Zodiatis, G.,Perivoliotis, L.,Fazioli, L.,Sorgente, R.,Manganiello, C., 2016. A multi-model assessment of the impact of currents, waves and wind in modelling surface drifters and oil spill. Deep Sea Research Part II: Topical Studies in Oceanography(133), 21-38.

Dhunny, A.Z., Lollchund, M.R., Rughooputh, S.D.D.V., 2015. Long-Term Wind Characteristics at Selected Locations in Mauritius for Power Generation.J.Wind Energy: doi.org/10.1155/2015/613936.

Dominicis, M. D., Bruciaferri,D., Gerin, R., Pinardi, N., Poulain, P.M., Garreau, P., Zodiatis, G., Perivoliotis, L., Fazioli, L., Sorgente, R., Manganiello, C., 2016. A multi-model assessment of the impact of currents, waves and wind in modelling surface drifters and oil spill. / Deep-Sea Research II 133, pp. 21–38.

Doorga, J.R.S., Chitna, D., Gooroochurn, O., Rawat, A., Ramchandure, V., Motah, B.A., Sunassee, S., Samayan, C., 2018. Assessment of the wave potential at selected hydrology and coastal environments around a tropical island, case study: Mauritius. Int. J. Ener. Environ. Eng. https://doi.org/10.1007/s40095-018-0259-7

Duran, R., Romeo, L., Whiting, J., Vielma, J., Rose, K., Bunn, A., Bauer, J., 2018. Simulation of the 2003 Foss Barge- Point Wells oil spill: A comparison between BLOSOM and GNOME oil spill models. J. Mar. Scie.Eng., 6, 104.

East, H.K., Perry, C.T., Beetham, E.P., Kench, P.S., Liang, Y., 2020. Modelling reef hydrodynamics and sediment mobility under sea-level rise in atoll reef island systems.Global and Planetary Change, 192, 103196.

Farzingohar, M, Zelina, Z, Yasemi, M., 2011.Oil spill modelling of diesel and gasoline with GNOME around Rajaee Port of Bandar Abbas, Iran. Iran. J. Fish. Sci., 10(1), pp. 35–46

Fingas, M., Brown, C., 2018. A review of oil spill remote sensing. Sensors 18, 1–18.

Fingas, M., Brown, C., 2014. Review of oil spill remote sensing. Mar. Pollut. Bull. 83, 9–23.

French-McCay, D.P., Jayko, K., Li, Z., Horn, M., Kim, Y., Isaji, T., Crowley, D., Spaulding, M., Decker, L., Turner, C., Zamorski, S., Fontenault, J., Shmookler, R., Rowe, J.J., 2015. Technical Reports for Deepwater Horizon Water Column Injury Assessment– WC_TR14: Modeling Oil Fate and Exposure Concentrations in the Deepwater Plume and Cone of rising Oil Resulting from the Deepwater Horizon Oil Spill. DWH NRDA Water Column Technical Working Group Report. Prepared for National Oceanic and Atmospheric Administration by RPS ASA, South Kingstown, RI, USA (September 29, 2015. Administrative Record no.DWH-AR0285776.pdf).

Garcia-Pineda, MacDonald, I.R., Li, X., Jackson, C.R., Pichel, W.G., 2012. Oil spill mapping and Measurement in the Gulf of Mexico with textural classifier neural network algorithm (TCNNA). IEEE J. Sel. Top. Appl. Earth Observ. Remote Sens. 6 (6), 2517–2525.

Garcia-Pineda, O., Holmes, J., Rising, M., Jones, R., Wobus, C., Svejkovsky, J., Hess, M., 2017. Detection of oil near shorelines during the deepwater Horizon oil spill using synthetic aperture radar (SAR). Remote Sens. 9 (6). https://doi.org/10.3390/rs9060567.

GNOME, 2012. General NOAA Operational Modeling Environment (GNOME) Technical Documentation. NOAA Technical Memorandum NOS OR&R 40. Seattle, Washington October 2012.

Guo, W.J., Wang, Y. X., 2009. A numerical oil spill model based on a hybrid method. Mar. Pollut. Bull. 58, pp. 726–734.

ITOPF (Oil Tanker Spill Statistics), 2019. The international tanker owners pollution federation.https://www.itopf.org/fileadmin/data/Documents/Company_Lit/Oil_Spill_Stats_brochure_2020_for_web.pdf.

Jones, H.F.E., Poot, M.T.S., Mullarney, J.C., de Lange, W.P., Bryan, K.R., 2016. Oil dispersal modelling: reanalysis of the Rena oil spill using open-source modelling tools. New Zealand Journal of Marine and Freshwater Research, 50(1), 10–27.

Kim, C.S., Cho, Y.K., Choi, B.J., Jung, K.T., You, S.H., 2013. Improving a prediction system for oil spill in the Yellow Sea: Effect of tides on the subtidal flow. Mar. Pollut. Bull., Marine Pollution Bulletin 68, 85-92.

Kim, D., Yang, G.G., Min, S., Hoh, C.H., 2014a. Social and ecological impacts of the *Hebei Spirit* oil spill on the west coast of Korea: Implications for compensation and recovery. Ocean and Coastal Management 102, pp. 533-544.

Kim, T.H., Yang, C.S., Oh, J.H., Ouchi, L., 2014b. Analysis of the contribution of wind factor to oil slick movement under the strong tidal condition: Hebei Sprit oil spill case. PLOS ONE, 9(1), e87393. doi:10.1371/journal.pone.0087393.

Kujawinski, E.B., Kido Soule, M.C., Valentine, D.L., Boysen, A.K., Longnecker, K., Redmond, M.C., 2011. Fate of dispersants associated with the Deepwater Horizon oil spill. Environ. Sci. Technol. 45, pp. 1298–1306.

Lee, K.H., Kim, T.G., Cho, Y.H., 2020. Influence of Tidal Current, Wind and Wave in Hebei Sprit oil spill modelling. J. Mar. Sci. Eng., 8, 69.

Lewis, D., 2020. Cleaning up after Mauritius oil spill. Nature 585, 172.https://doi.org/10.1038/d41586-020-02446-7.

Li, Y., Yu, H., Wang, Z.Y., Li, Y., Pan, Q.Q., Meng, S.J., Yang, Y.Q., Lu, W., Gua, K.X., 2019. The forecasting and analysis of oil spill drift trajectory during the Sanchi collision accident, East China Sea. Ocean Engineering 187, 106231.

Lutz, W., Wils, A. B., 1994. People on Mauritius: 1638–1991. In Population Development Environment., 75-97. Springer, Berlin, Heidelberg.

Mao, Y., Heron ML. 2008. The influence of fetch on the response of surface currents to wind studied by HF ocean surface radar. J Phys Oceanogr. 38(5):1107–1121.

Mariano, A.J., Kourafalou, V.H., Srinivasan, A., Kang, H., Halliwell, G.R., Ryan, E.H., Roffer, M., 2011. On the modelling of the 2010 Gulf of Mexico oil spill**.** Dyn. Atmos. Ocean., 52, 322-340, 10.1016/j.dynatmoce.2011.06.001

Maslo, A., Panjan, J., Zagar, D., 2014. Large-scale oil spill simulation using the lattice Boltzmann method, validation on the Lebanon oil spill case. Mar. Pollut. Bull, 84 (1–2), pp. 225-235.

Mezic, I., Loire, S., Fonoberov, V.A., Hogan, P., 2010. A New Mixing Diagnostic and Gulf Oil Spill Movement. Science, 330, 486-489.

Migliaccio, M., Nunziata, F., Buono, A., 2015. SAR polarimetry for sea oil slick observation. Int. J. Remote Sens. 36, 3243–3273.

Montiel, F., Squire, V., Doble, M., Thomson, J., Wadhams, P., 2018. Attenuation and directional spreading of ocean waves during a storm event in the autumn Beaufort Sea marginal ice zone. Journal of Geophysical Research: Oceans, 123, 5912–5932. https://doi.org/10.1029/2018JC013763

Naz,S., Iqbal, M.F., Mahmood, I.,Allam, M., 2021. Marine oil spill detection using Synthetic Aperture Radar over the Indian Ocean. Marine Pollution Bulletin, 162, 111921.

Nissanka, I, D., Yapa, P, D., 2017. Oil slicks on water surface: Breakup, coalescence, and droplet formation under breaking waves. Mar. Pollut. Bull., Marine Pollution Bulletin 114, pp. 480–493.

NOAA, 2020. UPDATED: NOAA Continues to Provide Remote Technical Assistance in Mauritius Oil Spill Response.https://response.restoration.noaa.gov/noaa-assist-oil-spill-mauritius.

Pan, Q., Yu, H., Daling, P.S., Zhang, Y., Reed, M., Wang, Z., Li, Y., Wang, X., Wu, L., Zhang, Z., Yu, H., Zou, Y., 2020. Fate and behaviour of Sanchi oil spill transported by the Kuroshio during January–February 2018. Mar. Pollut. Bull., Marine Pollution Bulletin 152, 110917.

Peterson, C.H., Rice, S.D., Short, J.W., Esler, D., Bodkin, J.L., Ballachey, B.E., Irons, D.B., 2003. Long-term ecosystem response to the Exxon Valdez oil spill. Science 302, pp. 2082–2086.

Pisano, A., De Dominicis, M., Biamino, W., Bignami, F., Gherardi, S., Colao, F., Coppini, G., Marullo, S., Sprovieri, M., Trivero, P., Zambianchi, E., Santoleri, R., 2016. An oceanographic survey for oil spill monitoring and model forecasting validation using remote sensing and in situ data in the Mediterranean Sea. Deep Sea Research Part II: Top. Stud. Oceanogr., 133, 132-145.

Pradhan, B., Das, Pradhan, C., 2020. Forecasting oil spill movement through trajectory modelling: a case study from Bay of Bengal, India. Model. Earth Syst. Environ. https://doi.org/10.1007/s40808-020-00933-4.

Prasad, S.J., Balakrishna Nair, T.M., Francis, P.A., Vijayalakshmi, T., 2014. Hindcasting and Validation of Mumbai Oil Spills using GNOME.Int. Res. J. Environment Sci.3 (12), pp.18-27.

Prasad, S.J., Balakrishnan Nair, T.M., Rahaman, H., Shenoi, S.S.C., Vijayalakshmi, T., 2018. An assessment on oil spill trajectory prediction: a case study on oil spill off Ennore Port. J. Earth Syst. Sci. 127:111.

Press Report: anytime. https://www.nytimes.com/2020/08/28/us/mauritius-dolphin-deaths.html.

Press Report: CBS News, 2020a. https://www.cbsnews.com/news/mauritius-oil-spill-tanker-ship-breaks-up/

Press Report: CBS News, 2020b. https://www.cbsnews.com/news/mauritius-oil-spill-sea-life-dying-endangered-species/.

Press Report: news18. https://www.news18.com/news/world/japanese-ship-involved-in-mauritius-oil-spill-breaks-apart-2791641.html

Press Report: Scientific American. https://www.scientificamerican.com/article/mauritians-launch-rescue-to-save-wildlif e-from-oil-spill/

Press Report: The India Express. August 11, 2020. https://indianexpress.com/article/trending/trending-globally/mauritius-oil-spill-from-donating-hair-to-building-floating-booms-locals-helping-in-crisis-6550096/

Rajendran, S., Vethamony, P., Sadooni, F.N., Al-Kuwari, H, Al-Khayat, J.A., Seegobin, V.O., Govil, H., Nasir, S., 2021. Detection of Wakashio oil spill off Mauritius using Sentinel-1 and 2data: Capability of sensors, image transformation methods and mapping. Environmental Pollution 274, 116618. https://doi.org/10.1016/j.envpol.2021.116618.

Reed, M., Turner, C., Odulo, A., 1994. The role of wind and emulsification in modelling oil spill and surface drifter trajectories. Spill Science and Technology Bulletin, 1(2), 143–157.

Rohrs, J., Dagestad, K.F., Asbjørnsen, H., Nordam, T., Skancke, J., Jones, C.E., Brekke, C., 2018. The effect of vertical mixing on the horizontal drift of oil spills. Ocean Sci., 14, 1581-1601.

Singh, A., Asmath, H., Chee, C.L., Darsen, J., 2015. Potential oil spill risk from shipping and the implications for management in the Caribbean Sea. Mar. Pollut. Bull, 93(1-2), pp. 217-227.

Spaulding, M.L., 2017. State of the art review and future directions in oil spill modelling. Mar. Pollut. Bull., 115, pp. 7-19.

Stokes, G. G., 1847: On the theory of oscillatory waves. Trans. Cambridge Phil. Soc., 8, 441–455.

Stolzenbach, K., Madsen, O.S., Adams, E.E., Pollack, A.M., Cooper, C.K., 1997. A Review and Evaluation of Basic Techniques for Predicting the Behavior of Surface Oil Slicks. Cambridge: Rep. 22, Dep. of Civ. Eng., Mass. Inst. Of Technol.

Suneel, V., TrinadhaRao, V., Gopika, S., Aditya, C., Vethamony, P., Ratheesh, R., 2019. Oil pollution in the Eastern Arabian Sea from invisible sources: A multi-techniques approach. Mar. Pollut. Bull., 146, pp. 683-695.

Suresh, G., Melsheimer, C., Korber, J.H., Bohrmann, G., 2015. Automatic estimation of oil seep locations in synthetic aperture radar images. IEEE Trans. Geosci. Remote Sens. 53 (8), 4218–4230.

Tang CL, Perrie W, Jenkins AD, DeTracey BM, Hu Y, Toulany B, Smith PC. 2007. Observation and modeling of surface currents on the grand banks: a study of the wave effects on surface currents. J Geophys Res. 112(C10): C10025

The National Crisis Committee (NCC). Update on Wakashio Vessel as at 4 pm on Monday, August 24. 2020. Available online: https://environment.govmu.org/Documents/wakashio/Press%20Release%20FINAL%20Wakashio%20as%20at%204PM%20 on%20Monday%20August%2024,%202020.pdf

Tian, S., Huang, X., Li, H., 2017. A new method to calibrate the Lagrangian model with ASAR images for oil slick trajectory, Mar. Pollut. Bull., Marine Pollution Bulletin, 116, (1-2), 95-102.

Topouzelis, K., Singha, S., Kitsiou, D., 2016. Incidence angle Normalization of Wide Swath SAR Data for Oceanographic Applications. Open Geosciences, 8(1), pp. 450-464. DOI: 10.1515/geo-2016-0029

Tuomi, L., Piikkio, O.V., Alenius, P., Bjorkqvist, J.V., Kahma, K.K., 2018. Surface stokes drift in the Baltic Sea based on the modelled wave spectra. Ocean Dynamics 68, 17–33.

Vethamony, P., Sudheesh, K., Babu, M.T., Saran, A. K., Mani Murali, R., Rajan, B., Srivastava, M., 2007. Trajectory of an oil spill off Goa, eastern Arabian Sea: Field observation and simulation, Environmental Pollution 148(2), 438-444.

World Bank Group, 2017. The Ocean Economy in Mauritius. Conference Edition.

Xu, Q., Cheng, Y., Liu, B., Wei, Y., 2015. Modelling of oil spill beaching along the coast of the Bohai Sea, China. Front. Earth Sci, 9(4), pp. 637–641.

Yao, F., Johns, W.E., 2010. A HYCOM modelling study of the Persian Gulf. 2. Formation and export of Persian Gulf Water. J. Geophys. Res., 115, p. C11018, 10.1029/2009JC05788

Yim, U.H., Khim, J.S., Kim, M., Jung, J.H., Shim, W.J., 2017.Environmental Impacts and Recovery After the Hebei Spirit Oil Spill in Korea. Archives of Environmental Contamination and Toxicology, 73, pp. 47–54.

Zelenke, B., O'Connor, C., Barker, C., Beegle-Krause, C.J., Eclipse, L (eds)., 2012. General NOAA Operational Modeling Environment (GNOME) Technical Documentation.US Dept. of Commerce, NOAA Technical Memorandum NOS OR&R 40. Emergency Response Division, NOAA, Seattle. WA: Emergency Response Division, NOAA. Pp. 105.https://response.restoration.noaa.gov/gnome_manual.

Zelenke, B., O'Connor, C., Barker, C., Beegle-Krause, C.J., Eclipse, L., 2012. General NOAA Operational Modeling Environment (GNOME). Technical Documentation, Seattle.

Zhao, J., Temimi, M., Al Azhar, M., Ghedira, H., 2015. Satellite-based tracking of oil pollution in the Arabian Gulf and the Sea of Oman. Can. J. Remote. Sens. 41,113–125.

Zhu, Z., Waterman, D.M., Garcia, M.H., 2018. Modelling the transport of oil–particle aggregates resulting from an oil spill in a freshwater environment. Environ Fluid Mech18, pp.967–984.